

1 **Estimation of structural steel and concrete stocks and flows at**
2 **urban scale – towards a prospective circular economy**

3 Atta Ajayebi^{a*}, Peter Hopkinson^a, Kan Zhou^b, Dennis Lam^b Han-Mei Chen^c, and
4 Yong Wang^c

5
6 ^aExeter Business School, University of Exeter, Northcote House, The Queen’s Drive,
7 Exeter, EX4 4QJ, UK

8 ^bDepartment of Civil and Structural Engineering, University of Bradford, Bradford,
9 West Yorkshire, BD7 1DP, UK

10 ^cSchool of Mechanical, Aerospace and Civil Engineering, University of Manchester,
11 Oxford Rd, Manchester, M13 9PL, UK

12 * Corresponding author

13 **Abstract:**

14 Quantification of stocks and flows of construction materials is a key first stage in
15 assessing the potential for creating higher value at end-of-life decisions compared to
16 destructive demolition. Steel and concrete are among the most widely used
17 construction materials primarily in structural components. Such components are
18 highly variable in design, type, and dimensions. In the absence of urban-scale
19 digitised models of structural components or building plans, accurate assessment
20 relies on either onsite inspection or modelling by material intensity (MI) co-efficient
21 which can vary by up to a factor of 100. In this study, we extend previous stock
22 modelling approaches through the development of a method that relies on building
23 archetypes and produces MI coefficients of steel and concrete that are
24 representative of frame types, temporally explicit and disaggregated at product level.
25 This is compared to the common existent method of calculating MI to demonstrate
26 the capabilities of the proposed method. Coupled with a spatiotemporal model of
27 urban buildings, the developed MI of both methods are applied to a case study in the
28 UK. The total in-use stock of steel and concrete within multi-storey buildings is
29 estimated at 81,000 tonnes and 655,000 m³ respectively. The stocks of steel and
30 concrete are disaggregated based on their functions as products, for instance steel
31 beams are distinguished from reinforcement steel. Subsequently, the embodied
32 carbon of the in-use stock is calculated as 350 kt CO₂eq. The results show the
33 proposed method enables a more granular assessment of the embodied carbon of
34 the structural material quantities.

35

36 1. Introduction:

37 Structural materials, notably steel, concrete and brick make up the major stocks of
38 building materials by volume and embodied carbon while resulting in substantial
39 flows of construction and demolition wastes. Globally The total in-use stock of steel
40 and concrete were 25.7 and 315.8Gt respectively in 2010 (Krausmann et al., 2017).
41 In the UK – the focus of this paper, the in-use built environment is estimated to
42 contain more than 5 billion tonnes of concrete and 500 million tonnes of steel.
43 Annually 247Mt of aggregates (MPA, 2018), 82 Mt of concrete and 5Mt of bricks
44 (BEIS, 2020) are used in the UK. Non-metallic mineral-based construction materials
45 alone were estimated to be responsible for over 10Mt of carbon emissions in 2018
46 (MPA, 2018). In 2017, 57 million tonnes of concrete and 12 million tonnes of steel
47 were in the demolition outflows (Streeck et al., 2020).

48 Structural products and materials are invariably long-lasting. Globally around 80% of
49 existing buildings were constructed before 1990, and half of them before 1960
50 (Pomponi and Moncaster, 2017). This trend of stock accumulation indicates the
51 significant volumes of the materials within buildings and their potentially diverse
52 characteristics. A growing body of research has studied and developed stock-flow
53 models for specific materials, types, and scales (Krausmann et al., (2017), Haas et
54 al., (2020), Stephan and Athanassiadis, (2017a)). These stocks open the possibility
55 of mining building products, components, and pure materials in the future, using new
56 forms of deconstruction over destructive demolition. However, urban buildings are
57 invariably downcycled into lower grade products and materials or landfilled at the
58 point of demolition when a building reaches the end of its service life – often well
59 before the end of technical life of the majority of materials and products (Pomponi
60 and Moncaster, 2017). Moreover, some of the biggest barriers to reclaim and re-use
61 of building structural materials is the lack of match between supply and demand of
62 reusable components. This requires a data registration and exchange database for
63 materials, standard components, and products from multiple existing buildings and
64 from which components for a new build can be sourced. This in turn requires
65 detailed and accurate information of exactly what and when reusable components
66 are available from End-of-Service-Life(EOSL) of buildings. Whilst various building
67 component marketplace exists these are mostly for non-structural components (e.g.
68 Salvo, (2020)), waste materials during/after the construction process (e.g.
69 Enviromate, (2020)), excessive materials (e.g. Excess materials exchange, (2020)
70 or excavation materials (e.g. Rocks, (2020)).

71 Accurate stock-flow information of the product and material components of existing
72 buildings at the EOSL opens the potential to quantify the reclaim potential of future
73 products such as steel or concrete components, assess their future value material
74 streams and their potential carbon and environmental benefits via direct re-use,
75 remanufacture or higher quality recycling. There is increasing interest and evidence
76 of selective product and material reclaim and re-use, notably high value heritage
77 materials and interior products such as ceiling panels, certain metals, doors, carpet

78 tiles and timber (Stephan and Athanassiadis (2017a), Gallego-Schmid et al., (2020),
79 Romero Perez de Tudela et al., (2020)).

80 Urban mining of structural building products and materials has great potential for
81 future circular economy construction systems but faces a number of challenges.
82 These include: firstly, the technical feasibility of being able to separate and reclaim
83 products from buildings that were not originally designed for deconstruction.
84 Secondly, in the absence of detailed building plans, how to accurately estimate the
85 quantity, age and location of stocks and their potential future flows. Thirdly, to
86 determine potential drivers to incentivise greater interest, value, and uptake of end-
87 of-life structural products and materials.

88 For example clay bricks bound by cement mortar considered too difficult to separate
89 without damage (Gregory et al., 2004). Hence, despite an estimated 800 billion
90 tonnes of bricks in buildings worldwide (Streeck et al., 2020), and the UK using over
91 2 billion each year, little interest is in estimating their spatial or temporal distribution
92 for urban mining potential. In a recent paper, the authors address these three
93 challenges in relation to clay bricks bound by concrete mortar (Ajayebi et al., 2020),
94 highlighting new engineering techniques to separate cement mortar, a novel spatio-
95 temporal stock flow model to estimate the total number of individual structural bricks
96 at urban scale and their embodied carbon and GWP benefit from re-use. The ability
97 to estimate the number of bricks is possible due to their relatively standardised
98 dimensions and from the known external dimensions (footprint on the ground and
99 height) of visible external structures calculated via GIS analysis and geo-data
100 sources including Ordnance Survey maps, google earth etc.

101 At the EOSL of buildings, concrete is rarely reclaimed for re-use, but is typically
102 crushed or downcycled as construction aggregate. A high proportion of structural
103 steel >85% is recycled (BCSA, 2019) often to a lower grade steel (rebar) due to
104 mixing and contamination at the point of collection and reclaim. There is a market for
105 steel re-use and a number of case studies have shown the economic and
106 environmental potential of the direct re-use of steel frame buildings (Brütting et al.,
107 2019)(Sansom and Avery, 2014). In the UK reusing rates are slightly higher for steel
108 decking (10%) and structural hollow steel sections (7%). The remainder is mostly
109 recycled. Moreover, Steel and concrete dominate the embodied carbon (measured
110 as Global Warming Potential: GWP) impact of new constructions hence the ability to
111 selectively reclaim and re-use these products within new builds would make a
112 significant contribution to future zero-carbon and circular economy systems and as
113 a result it is essential to account for the embodied carbon of the in-use stock. For
114 example, our studies have shown increasing the share of reusing concrete blocks
115 and steel decking can decrease the average aggregated embodied GWP of these
116 materials by 27%and 21% respectively (Ajayebi et al., 2020).

117 Compared to brick, estimations for steel and concrete are complicated by the fact
118 that the majority of the structure (frames, floors, ceilings, foundations etc) comprising

119 these materials are hidden and the dimensions of the components are highly varied.
120 Previous studies have estimated quantities of steel and concrete by coming up with
121 Material Intensity (MI) coefficient of buildings.

122 In this paper we use the same spatiotemporal stock-flow 3D model (Ajayebi et al.,
123 2020) to estimate of stocks and flows of steel and concrete in buildings at urban
124 scale in the absence of building plans. The aim of this paper is to present a method
125 for quantification of steel and concrete MI and material stocks of buildings for a UK
126 case study at urban scale using an improved MI calculation and spatio-temporal
127 modelling techniques. The paper is novel and distinctive in three ways. Firstly, it
128 creates modelling building archetypes of steel and concrete frame types and their
129 dimensions to create representative component-specific MI. Secondly, it is
130 temporally dynamic, taking account of trends of frame types within the construction
131 sector through time. Thirdly, it provides an additional carbon and GWP sub-system
132 to enhance estimations of the embodied carbon of the in-use stocks.

133 The paper addresses three key research questions

- 134 1) In the absence of building plans, can we improve levels of accuracy for
135 estimating building structural steel and concrete MI by modelling building
136 frame archetypes?
- 137 2) Can we apply spatiotemporal GIS and to quantify component-specific stocks
138 of steel and concrete material intensity at urban scale (thousands of buildings
139 rather than tens)?
- 140 3) What is the embodied carbon of these in-situ concrete and steel products and
141 materials?

142 The structure of the paper is firstly to describe approaches to modelling building
143 material stock-flows and previous studies on concrete and steel. Secondly, to
144 describe the spatio-temporal model and two different methods to estimating MI.
145 Thirdly to report findings and results. Finally, to discuss conclusions and future
146 research requirements.

147 **2. Background: Stock flow models for building products and materials**

148 Stock-flow models are designed to estimate the stocks of buildings and their rate of
149 accumulation or decline through time. The bottom-up stock assessment approach
150 attempts to account for buildings within urban areas by incorporating multiple
151 sources of data such as spatial land use datasets, construction records, models of
152 buildings, and direct data collection (Augiseau and Barles, 2017). Such approaches
153 connect geometrical aspects of structures to quantities of material stock, typically via
154 an MI coefficient. Calculation of the stocks via MI involves describing the stock
155 accumulation by using a representative unit, such as floor area or volume of
156 buildings, as a proxy for the inventory of in-use materials. It is then possible to
157 estimate the total quantity by multiplying the inventory with a known ratio of material
158 quantity per unit of inventory that is the MI (Gontia et al., (2018), Heeren and

159 Fishman, (2019)). As a result, by combining a spatial model of buildings and
160 appropriate set of MI, the quantities of materials can be estimated and mapped at
161 building level or wider urban scale. Wide-scale bottom-up assessment of material
162 stocks benefit from implementation of spatial analysis as it facilitates and enhances
163 the quality of results. Assigning location information and geometry of buildings that
164 can be analysed by Geographical Information Systems (GIS) will add the spatial
165 dimension to the analysis (Lanau et al., (2019), Miatto et al., (2019)).

166 The ideal data for estimating MI is via building plans or digitised models. This would
167 provide the precise dimensions of each components and would allow for accurate
168 calculation of quantities and dimensions of materials and products. For instance,
169 Building Information Modelling (BIM) has been used at the level individual buildings
170 for both material quantity assessment and accounting for embodied carbon (Cang et
171 al., 2020). For the majority of legacy buildings and pre-BIM, digitised building plans
172 are unavailable. Hence modelling of individual buildings and their components at
173 scale is not normally feasible. The few studies that have attempted this relied on
174 extensive primary data collection (e.g. Moynihan and Allwood, (2014)). To show the
175 difficulty of remote analysis, we conducted a pilot study to determine the feasibility
176 and practicality of assessing the number of columns and beams and their
177 dimensions using representative dimensions based on gross floor area (GFA) and
178 expert judgement. A comparison of results for sample building and validation against
179 an actual building plan demonstrated this method was too uncertain (see
180 supplementary material S8 for details).

181 The bottom-up approach faces a number of challenges. Firstly, statistical data on in-
182 use building material stocks are scarce, often of poor highly, heterogenous in
183 composition and hard to link to physical properties (Wiedenhofer et al., 2015). Hence
184 despite patterns of homogeneity in some structures (such as mass-produced council
185 flats or housing estates) there is often great variation in MI even at small-scale urban
186 studies. For the sake of practicality, bottom-up studies therefore tend to rely on
187 estimations using building 'archetypes' to represent groups of buildings (Augiseau
188 and Barles, 2017). By considering representative archetype buildings, it is possible
189 to assess in-use stocks over relatively larger areas. For instance, a study of
190 European buildings by Nemry et al., (2008), generated 53 archetypes of residential
191 buildings representing 80% of the in-use residential buildings in Europe where
192 buildings are classified based on construction decades and for each archetype
193 quantities of construction materials are recorded. Studies using a bottom-up
194 approach increasingly use spatial dimensions of buildings in urban-scale maps as
195 basis to associate the material quantities of archetypes to modelled buildings. Two
196 notable spatial features that most studies apply are Gross Floor Area (GFA) and
197 Volume. Both GFA and volume had the advantage of being available at cadastre-
198 level spatial datasets that cover large urban areas. GFA -or for earlier studies simply
199 the buildings footprint on the ground- has been used primarily because 2D records
200 and maps of individual buildings existed at urban and country scale for decades.

201 Recent developments in 3D GIS, LIDAR mapping, and satellite imagery provided the
202 opportunity of accessing location-specific data of volumes of constructions that can
203 be used as a basis to estimate the quantities of construction materials. The main
204 advantage of volumetric MI is that it can be associated with 3D maps so that can be
205 more accurately modelled due to being an external feature that can be mapped at
206 urban scale.

207 A second challenge is that most studies only focus on aggregated masses of the
208 materials for the entire buildings (Augiseau and Barles, 2017), rather than
209 disaggregated into products and structures (Stephan and Athanassiadis, (2017a),
210 Graedel et al., 2011)). Studies such as Nemry et al. (2018) have differentiated
211 between the forms and functions of materials within building structures such as
212 internal and external walls. However, the level of disaggregation in almost all
213 previous studies is between 'materials' rather than 'products' or 'components'. For
214 instance, concrete in the sub structure is not distinguished from vertical load-bearing
215 concrete and all concrete quantities are accounted as total mass or volumes.
216 Similarly, steel reinforcement (rebar) is not distinguished from load-bearing steel
217 beam products.

218 Thirdly, in order to produce high-resolution results, MI is usually applied in a
219 'temporally-static' manner such as tonnes of steel per volume of building regardless
220 of the time of construction (Wiedenhofer et al., 2019). Building design and stocks of
221 specific frame types and materials will vary through time. Hence, in order to assess
222 stocks of concrete or steel it is important to account for this dynamic when defining
223 MI of the buildings, particularly for multi-storey buildings where the choice of the load
224 bearing structure would have a great impact on the MI as it is evident from
225 comparative studies of steel-framed vs concrete-framed buildings (Wang et al.,
226 2015). Some studies account for the temporal dynamics by defining archetypes for
227 epochs (Mastrucci et al., 2017), but this may not be enough as the trends of the
228 construction industry change often rapidly (BCSA, 2019). This study proposes a
229 temporally dynamic approach where the year-by-year market share trends in steel
230 versus concrete frames are embedded in the calculation of MI.

231 Fourthly, mapping embodied carbon at urban scale was limited by aggregated
232 accounting of materials.

233 A few of the previous bottom-up stock assessments included mapping embodied
234 carbon of the in-use materials which can be instrumental for understanding the
235 impact of embodied carbon on the urban interactions or support carbon reduction
236 policies. (e.g. Stephan and Athanassiadis, (2017b), Mastrucci et al., (2017), Romero
237 Perez de Tudela et al., (2020)). These studies considered several construction
238 materials, but for practicality used aggregated accounting for materials. None of the
239 above studies considers building frame types and disaggregated material types into
240 their assessment. Calculating the embodied carbon of the in-use stock requires
241 linking the quantities of the materials and products to a Life Cycle Assessment

242 (LCA). As LCA is capable of accounting for a variety of steel and concrete products
243 with different qualities, if the stock assessment is capable of distinguishing between
244 the qualitative aspects of the stock, the quality and accuracy of LCA results will be
245 improved.

246 The wide variability of MI inputs and outputs makes it difficult to translate the findings
247 into large scale urban areas with confidence. To address this Ortlepp et al., (2018)
248 suggested in order to deal with the limitations of 'aggregated' MI for all buildings,
249 types of buildings and their components to be specified and separate material
250 composition indicators to be defined for each building component of each building
251 type. However, the task of defining elemental material and component indicators for
252 diverse varieties of buildings is an arduous work that requires designing and
253 calculating components of many structures. Previous studies have shown that
254 concrete-frame and steel-frame structures of similar dimensions and functions have
255 dissimilar compositions of quantities and types of steel and concrete (Wang et al.,
256 (2015), Xing et al., (2008)). GIS mapping can help to address this uncertainty by
257 adding a spatial dimension to the studies to deduce structural concrete and steel
258 dimensions and quantities based on the widths and depths of structures as it was
259 attempted by Stephan and Athanassiadis (2017b). However, despite accounting for
260 the dimensions of structural components, no study has mapped and considered the
261 different types of frames at urban-scale bottom-up assessment.

262 To address these various challenges and wide variations, this study applies a
263 method to integrate geospatial analysis, building frame archetypes, and temporal
264 trends of the construction industry into a stock-flow model. The following section
265 describes a method based on steel and concrete building frames and volumetric
266 calculation of MI to enable calculation of bills of materials, that are used as a basis
267 for our MI calculations. Section 3 will discuss how the MI of this study are calculated.

268

269 **3. Materials and methods**

270 **3.1. Overview:**

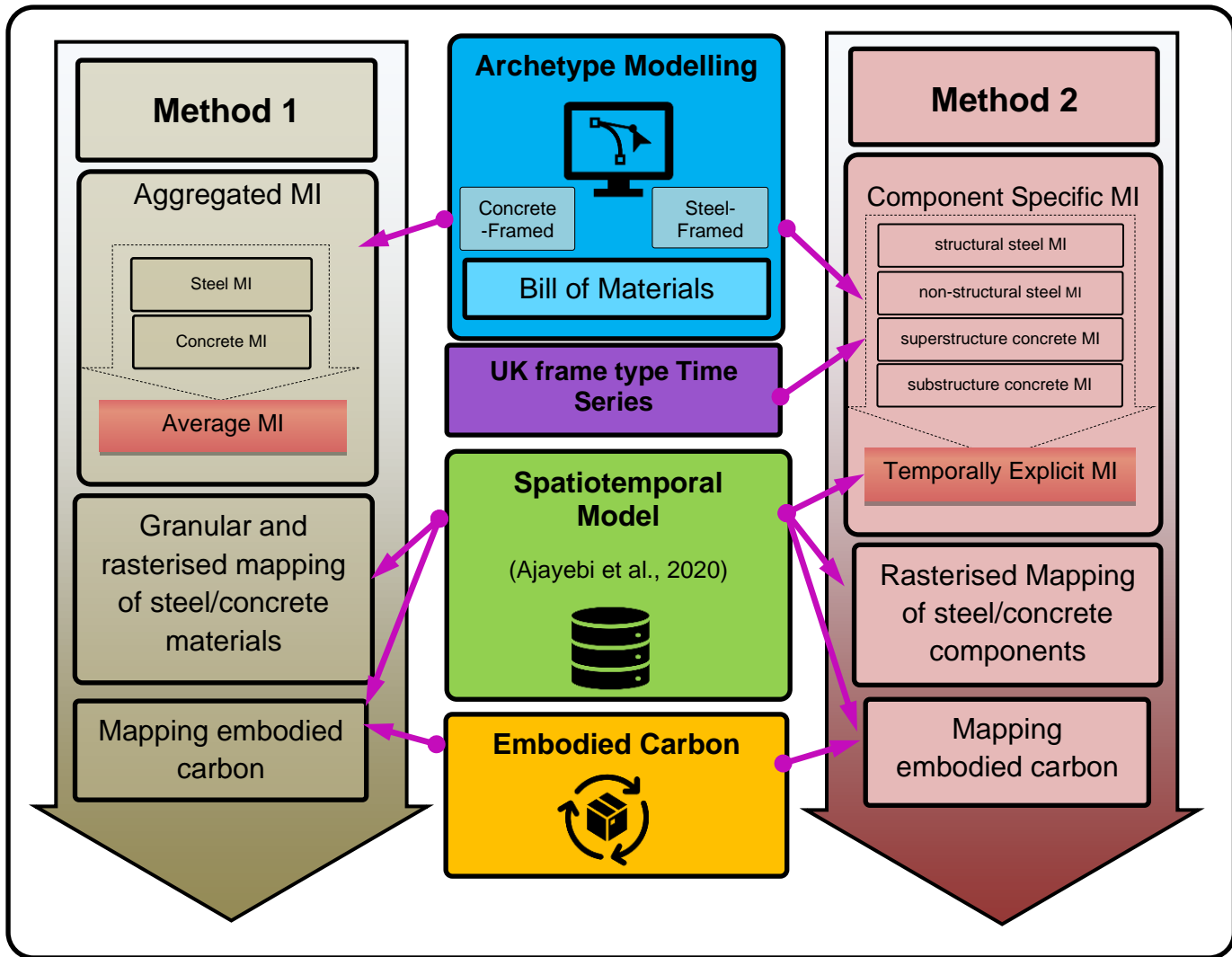
271 The structure of the methodology (Figure 3) is based on connecting a computer
272 modelling of archetypes, a spatiotemporal model previously reported by (Ajayebi et
273 al., 2020), and an LCA of the components of buildings in order to calculate relevant
274 MI, map in-use stocks of steel and concrete and their embodied carbon. This study
275 follows two methods. Method 1 is based on the existing approach of MI calculations
276 which has been used by the majority of previous bottom-up studies. Method 1 is
277 compared to the previous studies and it is also presented as a basis for comparison
278 to method 2, an improved method for calculating disaggregated and temporally
279 explicit MI in order to demonstrate the strengths and limitations of each method. For
280 this purpose, two representative multi-storey archetypes are modelled and used for
281 calculation of MI of both methods. One archetype represents a typical steel-framed

282 building and the other represents a typical concrete-framed building. For each
283 archetype, detailed bills of materials are calculated from the computer models
284 distinguishing between individual steel and concrete structural components.

285 For method 1, aggregated quantities of steel and concrete for each of the two
286 archetypes are calculated from the bills of materials regardless of the forms of the
287 structural components. These quantities (mass of steel and volume of concrete) are
288 divided into the building volumes in order to create a set of volumetric MI for each
289 archetype. Method 2 uses disaggregated bill of materials of each of the two
290 archetypes and categorises the steel and concrete quantities of structural
291 components into four groups of structural steel, non-structural steel, superstructure
292 concrete and substructure concrete. Subsequently, an intermediary volumetric MI is
293 calculated for each archetype. This intermediary MI is then extended by being
294 combined with the time-series data on frame types of construction of multi storey
295 buildings in the UK. This produces a representative year-specific MI.

296 For each method, the calculated MI are applied to the entire selected buildings of the
297 case study area and the results are mapped and the corresponding embodied are
298 calculated based on both methods and are compared.

299



300
301 *Figure 3: The framework of the model: procedures, methods, and data sources*

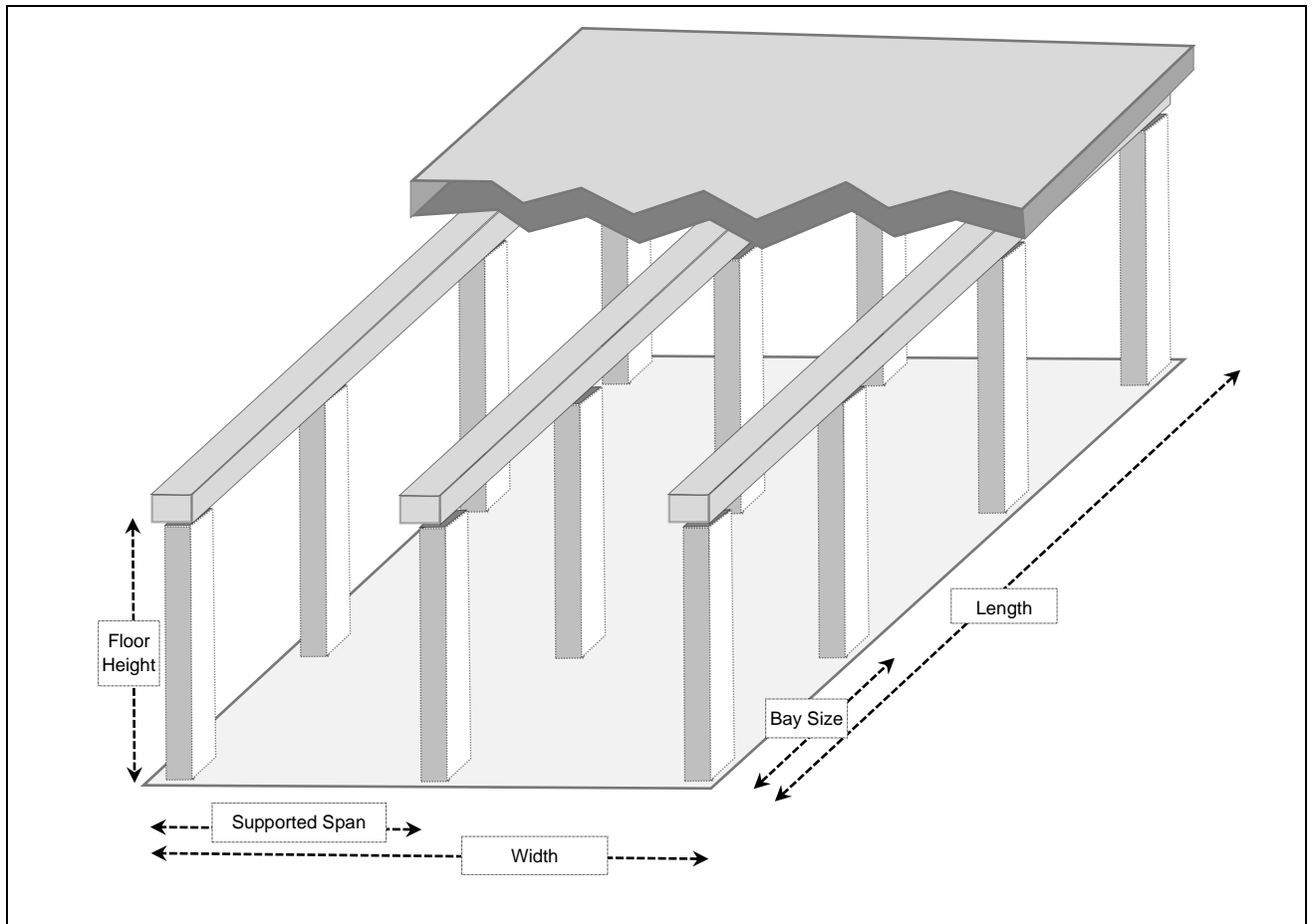
302 **3.2. Archetypes: Linking Steel-framed vs Concrete-framed archetypes and**
303 **material intensities:**

304 As it was explained before, modelling archetypes is a practical and accurate
305 approach for creating MI for certain building types. Here, based on the frame types,
306 two archetypes are modelled for multi-storey buildings, one for a steel-framed and
307 one for a concrete-framed building. The internal design of the components of each
308 archetype is taken into consideration. The specifications of these archetypes are
309 demonstrated in Table 1. Structural assemblies of foundations, walls, roofs, floors,
310 and structural frames are included in the archetypical analysis. Specifically, heavy
311 components of beams, columns, floor slabs, foundations, walls and light components
312 of rebar, rods, studs, screws, nuts, bolts, and wire mesh are included. The details of
313 the itemisation and specifications of the archetypes are provided in the
314 supplementary material (S1-S3). Computer representation of the mentioned steel
315 and concrete building components are modelled using the library of buildings of the
316 *Athena Impact Estimator V5.4*, based on their frame types as well as dimensions.
317 For each of the archetypes, the bills of materials are produced in both aggregated

318 (i.e. total mass of steel and total volume of concrete) and disaggregated (e.g.
 319 substructure concrete) forms. The former is used as input for method 1 and the latter
 320 as an input for method 2 described more fully in section 3.5.

321

322 *Table 1: Descriptions of the steel-framed and concrete-framed archetypes.*
 323 *These have been determined by considering two representative sample*
 324 *buildings of the existing archetypes.*



Archetypes		
Frame type	Steel-Framed	Concrete-framed
Building Height	12 m	9.2 m
Gross Floor Area	2000 m ²	1215 m ²
Footprint Area	500 m ²	405 m ²
Supported Span	9.1 m	6 m
No. floors	3	4
Volume	6000	3726
Live Load	3.6 kN/m ²	3.6 kN/m ²

325

326 **3.3. A spatio-temporal-type framework:**

327 The core of the spatiotemporal model is a GIS multilayer framework that has several
 328 clusters of data embedded into the map, integrating data on building geometries,
 329 locations, GFA, building volumes, year of construction and building types. This study
 330 is mounted on the 'REBUILD' model that was previously published in Ajayebi et al.
 331 (2020). More details about this model and its development are described in the
 332 article.

333 **3.4. Method 1: Applying static material intensities:**

334 The MI of method 1 are volumetric and are calculated by using the aggregated bills
 335 of materials of the two archetypes and dividing into the volumes of buildings. As a
 336 result, two sets of MI are produced, one would represent the steel-framed buildings
 337 and the other the concrete-framed buildings. Ideally, the MI set of the steel-framed
 338 archetype should be applied to the modelled buildings that are steel-framed and
 339 similarly for concrete-framed. However, the data about the type of structural frame of
 340 individual buildings is not available at granular urban scale in the UK and available
 341 surveys on building frame types are aggregated for all buildings at the national level
 342 (Housing Survey, 2017). As a result, an average UK MI is calculated based on a 50-
 343 50 share for each structural frame type for method1 in order to replicate the
 344 approach of previous studies and compare it to method2

345 The formula and details of calculations of volumetric MI are provided in the
 346 supplementary materials S4. The presented volumetric MI in table 2 are derived from
 347 the two archetypes and their aggregated bills of materials. Each volumetric MI
 348 describe the quantity of steel or concrete per m³ volume of the building. Based on
 349 the steel-framed and concrete-framed sets of MI, an average MI is calculated as
 350 16.67 kg/m³ for steel and 0.11 m³/m³ for concrete respectively. Table 2 highlights the
 351 differences in quantities and MI for concrete and steel depending on the frame type.
 352 A steel-framed building for example has a concrete MI 40% lower than a concrete
 353 framed building but a higher quantity of steel with a consequent 35% higher
 354 volumetric MI. The average MI represents all multi-storey buildings and is applied to
 355 all selected case study buildings.

356 *Table 2: Volumetric MI of the steel-framed and concrete-framed archetypes*
 357 *calculated by method 1*

Archetype: Steel-Framed	Quantities	Volumetric MI /m ³	Unit
Total Concrete in Building (m ³)	489	0.08	m ³ /m ³
Total Steel in Building (kg)	65,865	20.28	kg/m ³
Archetype: Concrete-Framed	Quantities	Volumetric MI /m ³	Unit
Total Concrete in Building (m ³)	535	0.14	m ³ /m ³
Total Steel in Building (kg)	48,684	13.06	kg/m ³
Average Building	-	Volumetric MI /m ³	Unit
Concrete (m ³)	-	0.11	m ³ /m ³
Steel (kg)	-	16.67	kg/m ³

358

359 The derived output is a set of MI for a representative building that is described as
360 mass and volumes of steel and concrete per volume of building. The MI are also
361 presented in the table 6 along with other studies that used similar methods for
362 comparison. Comparing to the previous studies, reveals that the calculated MI are in
363 line with the calculations of other studies. To demonstrate this, a comparison of the
364 steel MI of the method 1 of this study and another study that analyses the mean
365 value of more than a hundred previous studies (Heeren and Fishman, 2019) differs
366 by 16%, considerably lower than the variations of the studies that were reviewed in
367 Table 6.

368 Subsequently, the volumetric MI is then applied to all buildings in the case study
369 area on a spatiotemporal model, and granular maps of quantities of steel and
370 concrete are generated. The resolution of this map is at the level of individual
371 buildings.

372 **3.5. Method 2: Applying temporally explicit and component-specific material** 373 **intensities:**

374 For multi-storey buildings, the type of building frames is a pivotal factor in
375 determining the material content (BCSA, 2019). As a result, component level
376 assessment of steel and concrete components requires integration of frame types
377 into the analysis. Earlier in this paper we discussed data on frame types of individual
378 buildings is very limited in scope and reliability. However, instead of relying on
379 identifying frame types of individual buildings, the analysis can rely on generating
380 sets of MI that can be associated to the available qualities of buildings (e.g. year of
381 construction) and map component level stocks at urban level. This section focuses
382 on developing these MI sets.

383 Method 2 incorporates two sources of data: a) a disaggregated set of MI from the
384 two archetypes, and b) the data from a yearly survey of the market share of multi-
385 storey buildings. This facilitates generating MI that is both disaggregated for
386 construction components, and specific for each year of construction. Method 2 uses
387 the two archetypes that were described in section 2.2. While the bills of materials of
388 the two archetypes were aggregated for methods 1 and to total quantities are
389 described for steel and concrete, method 2 describes bills of materials as four
390 components-specific parts of: 1) substructure concrete, 2) superstructure concrete,
391 3) structural steel, and 4) non-structural steel. Substructure concrete encompasses
392 foundations and ramps while superstructure concrete includes walls, floors, roofs,
393 columns, and beams. Structural steel encompasses steel columns and beams while
394 non-structural steel consists of rebar, rods, studs, and light sections. By categorising
395 the bills of materials into 'components', the volumetric component-specific MI of each
396 archetype can be calculated. Details of the archetypes and their aggregated and
397 disaggregated bills of materials and MI are described in the supplementary material

398 S1-S3. The component-specific volumetric MI that are calculated from the two
 399 archetypes are displayed in table 3.

400 *Table 3: Volumetric component-specific MI of the steel-framed and concrete-*
 401 *framed archetypes*

component-specific MI	Substructure Concrete (m ³ /m ³)	Superstructure Concrete (m ³ /m ³)	Non-structural steel (kg/m ³)	Structural Steel (kg/m ³)
Steel-Framed (MI_s) Archetype	0.016	0.066	4.545	15.743
Concrete-Framed (MI_c) Archetype	0.026	0.118	13.066	0

402

403 The volumetric of MI of table 4 are used as an intermediary input to generate MI of
 404 method 2 that are both component specific and temporally explicit. For this purpose,
 405 time series of market trends of the construction industry in the UK in considered as a
 406 basis for generating the MI. A year-by-year survey of new constructions in the UK
 407 from 1970 onwards revealed that the vast majority (around 90%) of multi-storey
 408 buildings were either steel-framed or concrete-framed (BCSA, (2019), Housing
 409 Survey, (2017)). Steel-framed and concrete-framed buildings dominate the multi-
 410 storey construction sector (supplementary material S5). The other types of
 411 construction (e.g. self-sustaining masonry or timber-framed) account for only around
 412 10% of the constructions. The survey recorded the proportions of buildings based on
 413 the type of frames and the statistics shows that share of steel-frame buildings
 414 increased in the UK since 1980 and reached to above 70% of the market in the
 415 2000s. For the period of 1950-1970 when accurate data on the market shares of
 416 building frame types is not available, it is possible to estimate the market shares by
 417 defining representative tendency lines. The market trends seem to plateau in recent
 418 years that suggest a logarithmic function can define the contemporary and near
 419 future market saturation trends. However, for the period of 1950-1970 when
 420 historical data in unavailable, the authors believe the best representative
 421 retrospective correlation would be linear extrapolations representing a decline during
 422 the mentioned period, as it is depicted in figure 4.

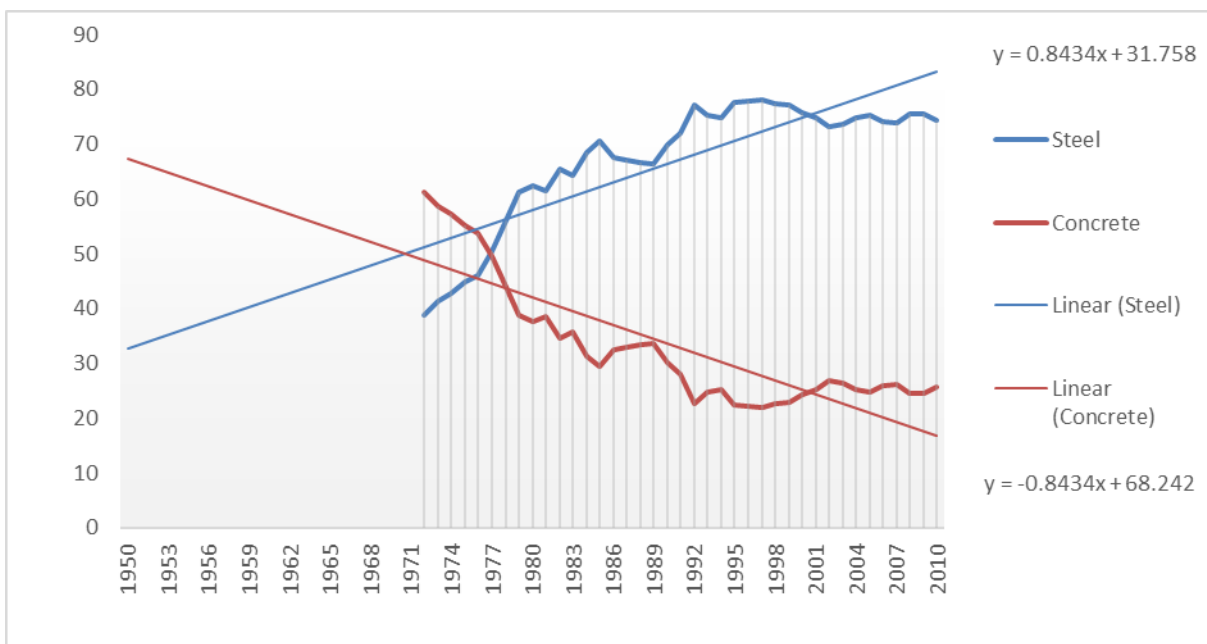
423 This data provides an opportunity to be associated with trends of constructions
 424 adding to the in-use stocks. For this purpose, two sets of material intensities that
 425 were calculated for steel-framed (MI_s) and concrete-framed (MI_c) archetypes are
 426 merged based on these shares, in order to estimate typical MI that are
 427 representative for all buildings of the selected temporal cohorts of construction years.
 428 The proportions of steel-framed and concrete-framed buildings are applied to create
 429 the temporally explicit MI by considering the annual share of construction frame type,
 430 as a result a year-specific MI can be calculated by:

431 EQ1:

$$MI_t = \frac{MI_S}{MI_C} * C_t$$

432 Where MI_t is the volumetric, component specific and spatially explicit material
433 intensity of year t , MI_S is the material intensity derived from an archetypical steel-
434 frame building, MI_C is the material intensity derived from an archetypical concrete
435 frame building, and C_t is the ratio of steel-frame over concrete-frame buildings in
436 year t . The MI values are time-dependent (yearly) and describe quantities of steel
437 and concrete components for per m^3 volume of each building. Despite nearly 10% of
438 the multi-storey buildings belonging to other types of frames (e.g. timber, masonry),
439 for the sake of practicality of the calculations, the share of steel and concrete frame
440 buildings is extrapolated to account for 100% of the market. In addition, as the data
441 is only available after 1980, linear trendlines are applied in order to create estimation
442 between 1950 and 1980. The data of the share of structure types and the trendlines
443 are demonstrated in Figure 4.

444



445
446

447 *Figure 4: The historical share (percentages) of multi-storey steel-frame,*
448 *concrete-frame, extrapolated to cover 1950-2010.*

449 Details of the temporally and component specific MI are described in the
450 supplementary material S5.

451 The MI table below (Table 4) demonstrates the calculated MI for years 1950-2018.
452 The results show for an average multi-storey building in the UK, total quantities of
453 concrete have been almost constantly decreasing from $0.15 m^3/m^3$ in 1950 to 0.09
454 m^3/m^3 in 2018, while the quantities of steel are increasing from $13 kg/m^3$ in 1950 to
455 $18.5 kg/m^3$ in 2018. The spatially explicit MI demonstrate that quantities of steel

456 products in multi storey buildings of the UK has been increasing almost steadily
 457 since 1950s with steepest increase being between 1970 and 1990. On the contrary,
 458 the concrete quantities have been decreasing since 1950s, but the decrease rate
 459 has been levelling off since 1990s.

460 *Table 4: The ratios of concrete-framed and steel-framed buildings and the*
 461 *calculated temporally explicit volumetric material intensities. Concrete and*
 462 *steel MI are in m³/m³ and kg/m³ respectively.*

Frames/ year			Material Intensity			
Year	Steel framed	Concrete framed	Substructure Concrete	Superstructure Concrete	Non-structural Steel	Structural Steel
Pre1950	5	95	0.025	0.116	12.640	0.787
1950	6.5	93.5	0.025	0.115	12.516	1.016
1951	7.3	92.7	0.025	0.115	12.444	1.149
1952	8.1	91.9	0.025	0.114	12.372	1.282
1953	9.0	91.0	0.025	0.114	12.300	1.415
1954	9.8	90.2	0.025	0.113	12.229	1.548
1955	10.7	89.3	0.024	0.113	12.157	1.680
1956	11.5	88.5	0.024	0.112	12.085	1.813
1957	12.4	87.6	0.024	0.112	12.013	1.946
1958	13.2	86.8	0.024	0.111	11.941	2.079
1959	14.0	86.0	0.024	0.111	11.869	2.211
1960	14.9	85.1	0.024	0.111	11.797	2.344
1961	15.7	84.3	0.024	0.110	11.725	2.477
1962	16.6	83.4	0.024	0.110	11.654	2.610
1963	17.4	82.6	0.024	0.109	11.582	2.743
1964	18.3	81.7	0.024	0.109	11.510	2.875
1965	19.1	80.9	0.024	0.108	11.438	3.008
1966	20.0	80.0	0.024	0.108	11.366	3.141
1967	20.8	79.2	0.024	0.107	11.294	3.274
1968	21.6	78.4	0.023	0.107	11.222	3.406
1969	22.5	77.5	0.023	0.107	11.150	3.539
1970	23.3	76.7	0.023	0.106	11.079	3.672
1971	24.2	75.8	0.023	0.106	11.007	3.805
1972	25.0	75.0	0.023	0.105	10.935	3.938
1973	25.9	74.1	0.023	0.105	10.863	4.070
1974	26.7	73.3	0.023	0.104	10.791	4.203
1975	27.5	72.5	0.023	0.104	10.719	4.336
1976	28.4	71.6	0.023	0.103	10.647	4.469
1977	29.2	70.8	0.023	0.103	10.576	4.601
1978	30.1	69.9	0.023	0.103	10.504	4.734
1979	30.9	69.1	0.023	0.102	10.432	4.867
1980	38.8	61.2	0.022	0.098	9.758	6.112

1981	41.4	58.6	0.022	0.097	9.540	6.514
1982	42.7	57.3	0.021	0.096	9.428	6.722
1983	44.9	55.1	0.021	0.095	9.236	7.076
1984	46.2	53.8	0.021	0.094	9.133	7.266
1985	50.5	49.5	0.021	0.092	8.759	7.958
1986	56.2	43.8	0.020	0.089	8.279	8.845
1987	61.2	38.8	0.020	0.086	7.853	9.631
1988	62.4	37.6	0.019	0.085	7.753	9.816
1989	61.4	38.6	0.020	0.086	7.830	9.674
1990	65.5	34.5	0.019	0.084	7.487	10.308
1991	64.2	35.8	0.019	0.085	7.596	10.107
1992	68.6	31.4	0.019	0.082	7.220	10.801
1993	70.6	29.4	0.019	0.081	7.051	11.113
1994	67.5	32.5	0.019	0.083	7.317	10.622
1995	67.1	32.9	0.019	0.083	7.352	10.557
1996	66.7	33.3	0.019	0.083	7.385	10.496
1997	66.3	33.7	0.019	0.083	7.416	10.438
1998	69.9	30.1	0.019	0.082	7.110	11.003
1999	72.0	28.0	0.019	0.080	6.927	11.342
2000	77.3	22.7	0.018	0.078	6.481	12.165
2001	75.3	24.7	0.018	0.079	6.651	11.852
2002	74.7	25.3	0.018	0.079	6.698	11.764
2003	77.5	22.5	0.018	0.077	6.460	12.205
2004	77.8	22.2	0.018	0.077	6.438	12.245
2005	78.0	22.0	0.018	0.077	6.418	12.283
2006	77.4	22.6	0.018	0.078	6.469	12.188
2007	77.2	22.8	0.018	0.078	6.490	12.150
2008	75.8	24.2	0.018	0.078	6.605	11.937
2009	74.7	25.3	0.018	0.079	6.698	11.764
2010	73.2	26.8	0.018	0.080	6.826	11.528
2011	73.6	26.4	0.018	0.080	6.792	11.591
2012	74.7	25.3	0.018	0.079	6.698	11.764
2013	75.3	24.7	0.018	0.079	6.651	11.852
2014	74.2	25.8	0.018	0.079	6.747	11.675
2015	73.9	26.1	0.018	0.079	6.772	11.629
2016	75.4	24.6	0.018	0.079	6.639	11.875
2017	75.6	24.4	0.018	0.079	6.626	11.899
2018	74.4	25.6	0.018	0.079	6.725	11.716

463

464 **3.6. Study area:**

465 The geographical scope of the study is the city of Bradford in Northern England, UK.

466 The study's focus is limited to multi-storey buildings. This is because load-bearing

467 masonry and timber frames dominate the structural components of single-storey
 468 building stock in England (English Housing Survey, 2018) so we decided to exclude
 469 single storey buildings from our analysis. Buildings are categorised into four classes
 470 of 1) commercial, 2) office, 3) low rise flats, and 4) high rise flats. These four classes
 471 are selected because of their anticipated higher contents of steel and concrete as
 472 the model developed by (Ajayebi et al., 2020) demonstrated that the vast majority of
 473 all multi-storey buildings in the case study area would fit into these four classes. Data
 474 on building dimensions, locations, and construction years are embedded in the
 475 model at the resolution of individual buildings. Information about the numbers of
 476 buildings of each type, footprint areas and GFA are presented in table 5.

477 *Table 5: The numbers and areas of the buildings and their types in the*
 478 *case study area. The three indicators of the buildings' dimensions are the*
 479 *footprint area, the gross floor area, and the relevant heights of buildings.*
 480 *The figures are derived from the spatiotemporal model of the case study*
 481 *area developed by (Ajayebi et al., 2020).*

			Building Footprint Area			Building Heights	
	No. buildings	Total Gross Floor Area (m ²)	Total Footprint Area (m ²)	Average Footprint Area (m ²)	stdv	Average Building Height (m)	stdv
Low rise	999	215,117	93,180	93.4	142.8	6.1	2.5
High Rise	35	87,932	10,024	294.8	187.1	23.5	8.6
Office	294	487,450	114,904	392.2	627.7	10.4	6.3
Commercial Core	1,147	1,104,555	377,306	329.2	821.5	8.6	4.8

482

483 Figure 5 demonstrates the boundaries of the case study area within the city of
 484 Bradford and the footprints of all buildings. The selected buildings that are included
 485 in our study are highlighted.



486

487 *Figure 5: The geographical scope of the study within the UK (above) and*
 488 *the modelled buildings (orange) compared to the footprints of all*
 489 *constructions in the case study area.*

490 **3.7. Mapping embodied carbon:**

491 As this study views materials as repositories for potential re-use, accounting for the
 492 embodied carbon can help understand the impact of different EOSL activities
 493 (including reclaiming and reusing) on the overall GHG emissions of constructions in
 494 order to meet carbon reduction goals. Due to the reuse-oriented perspective of this
 495 study, the production stage of the components that includes extraction of raw
 496 materials, manufacturing of products, and transportation are determining the
 497 embodied carbon of this study (BS, 2011). Operational GHG emissions (e.g.
 498 associated with heating spaces) are excluded. For this purpose, an LCA is
 499 performed with a focus of analysing the four 'components' of steel and concrete that

500 are specified in method 2. It should be noted that this LCA calculates the embodied
501 carbon of similar new products that are available on the market (AKA 'Carbon
502 Replacement Value'), instead of the quantities of the actual released emissions of
503 the in-use buildings at the time of production/ construction. The LCA is performed by
504 using the SimaPro tool (v8.5.2). The sources of life cycle inventory analysis data are
505 specified in the table S2 and the impact assessment of IPCC GWP 100a is applied.
506 The methodology of calculating the embodied carbon of each of the four products is
507 described in the Supplementary Material S6.

508 **3.8 Validation of Material Intensities:**

509 In this section we compare the calculated MI of this study to a normalised review of
510 previous studies in order to validate the calculated MI. Previous studies (see table 6
511 below) have estimated aggregated quantities of steel and concrete derived from the
512 of Material Intensity (MI) coefficient of buildings derived in two different ways, which
513 vary depending on the aims and scope of the study. The first approach applied MI
514 that was obtained and imported from developed models, studies, reports and look-up
515 tables (e.g. Tanikawa and Hashimoto, (2009), Heeren and Fishman (2019)). The
516 second approach is to directly calculate the MI based on the bills of materials of
517 certain modelled exemplar buildings (Gontia et al., (2018), Ortlepp et al., (2018)).
518 These can be in a form of real or modelled building 'archetypes' that are considered
519 to be representative of a certain similar group of buildings (e.g. Nemry et al 2018,
520 *ibid*). In another study, (Schebek et al., 2017) considered 19 individual buildings as
521 archetypes that their MI could represent groups of buildings based on their
522 construction decade or building type. As stated above, the type of frame can make a
523 significant difference to the estimation of overall MI. Hence this study presents a new
524 approach to MI calculation-based frame archetypes that allows calculating
525 disaggregated MI.

526 Table 6 summarises and highlights previous bottom-up approaches to estimating MI
527 of steel and concrete buildings. As it can be seen, there is a substantial variation in
528 MI range which supports a review by (Gontia et al., 2018) into the impact of MI on
529 the quantitative results of material stock assessment studies. This study
530 demonstrated that the MI of similar case studies and materials can vary up to
531 hundred-fold. It also demonstrated that the number of floors and the footprint size of
532 a building have a considerable impact on the MI of materials. As stated above, this
533 variation can be due to the wide variety of dimensions and types of the load-bearing
534 components especially of steel and concrete framed multi-storey buildings. As a
535 result, the architecture, footprint and the number of floors are impacting the material
536 quantities as various steel and concrete products are used. Such variations are often
537 neglected in the bottom-up assessments due to lack of data and as a consequence
538 MI in the stock-flow literature are highly context-specific and help explain the large
539 variation between different studies.

Table 6: A comparison of steel and concrete MI of multi-storey buildings of method1 of this study and previous studies of material stocks

Study	Building Type	MI and units		Case study	MI Source	MI type	Normalised MI	
		Concrete	Steel				Concrete m3/m2	Steel kg/m2
Wang et al., (2015)	Concrete-framed	-	43-65 kg/m ²	China	Calculated	2D GFA	-	75.5
	Steel-framed	-	55-100 kg/m ²				-	105
Xing et al., (2008)	Concrete-framed	0.79 m ³ /m ²	11.55 kg/m ²	Shanghai, China	Calculated	2D GFA	0.79	11.55
	Steel-framed	0.40 m ³ /m ²	61.51 kg/m ²				0.4	61.51
Dimoudi and Tompa, (2008)	Office: Concrete-framed-1	0.49 m ³ /m ²	47.33 kg/m ²	Athens, Greece	Calculated	2D GFA	0.49	47.33
	Office: Concrete-framed-2	0.71 m ³ /m ²	78.50 kg/m ²				0.71	78.5
Tanikawa and Hashimoto, (2009)	Brick base flat	146 kg/m ²	2 kg/m ²	Manchester, UK	Imported	2D Footprint	-	-
	Concrete block flat	524 kg/m ²	2 kg/m ²				-	-
	Reinforced concrete	397 kg/m ²	22 kg/m ²				-	-
Han and Xiang, (2013)	Residential urban	-	23-40 kg/m ²	China	Calculated	2D GFA	-	43
	Residential rural	-	4-6 kg/m ²				-	Na
Gontia et al., (2018)	Multi-family 80s	-	190 kg/m ²	Sweden	Calculated	2D GFA	-	190
	Multi-family 2000s	-	312 kg/m ²				-	312
Schebek et al., (2017)	Non-residential	50-840 kg/m ³	2-191 kg/m ³	Frankfurt, Germany	Calculated/Imported	Volumetric	-	-
Heeren and Fishman, (2019)	Residential	563.71 kg/m ²	48.42 kg/m ²	Multiple	Imported	2D GFA	0.24	48.42
	Non-residential	697.92 kg/m ²	27.42 kg/m ²				0.3	27.42
Ortlepp et al., (2018)	Commercial	75 kg/m ³	37 kg/m ³	Germany	Calculated	Volumetric	-	-
	Office	226 kg/m ³	23 kg/m ³				-	-
Ortlepp et al., (2016)	Office	1.3 t/m ²	0.12 t/m ²	Germany	Calculated	2D GFA	0.56	120
	Institutional	1.1 t/m ²	0.09 t/m ²				0.47	90
This study	Concrete-framed	0.44 m ³ /m ²	40.07 kg/m ²	Bradford UK	Calculated	2D GFA	0.44	40.07
	Steel-framed	0.24m ³ /m ²	60.86 kg/m ²				0.24	60.86
	Concrete-framed	0.14 m ³ /m ³	13.06 kg/m ³			Volumetric	-	-
	Steel-framed	0.08 m ³ /m ³	20.28 kg/m ³				-	-

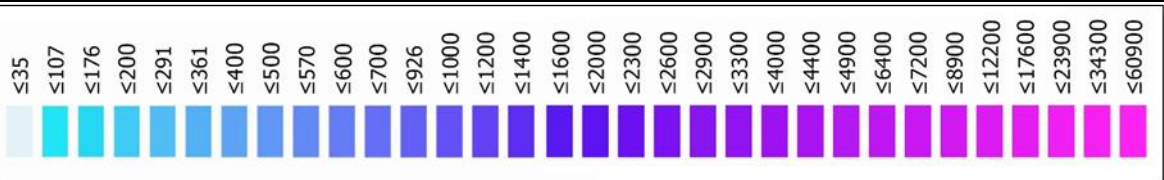
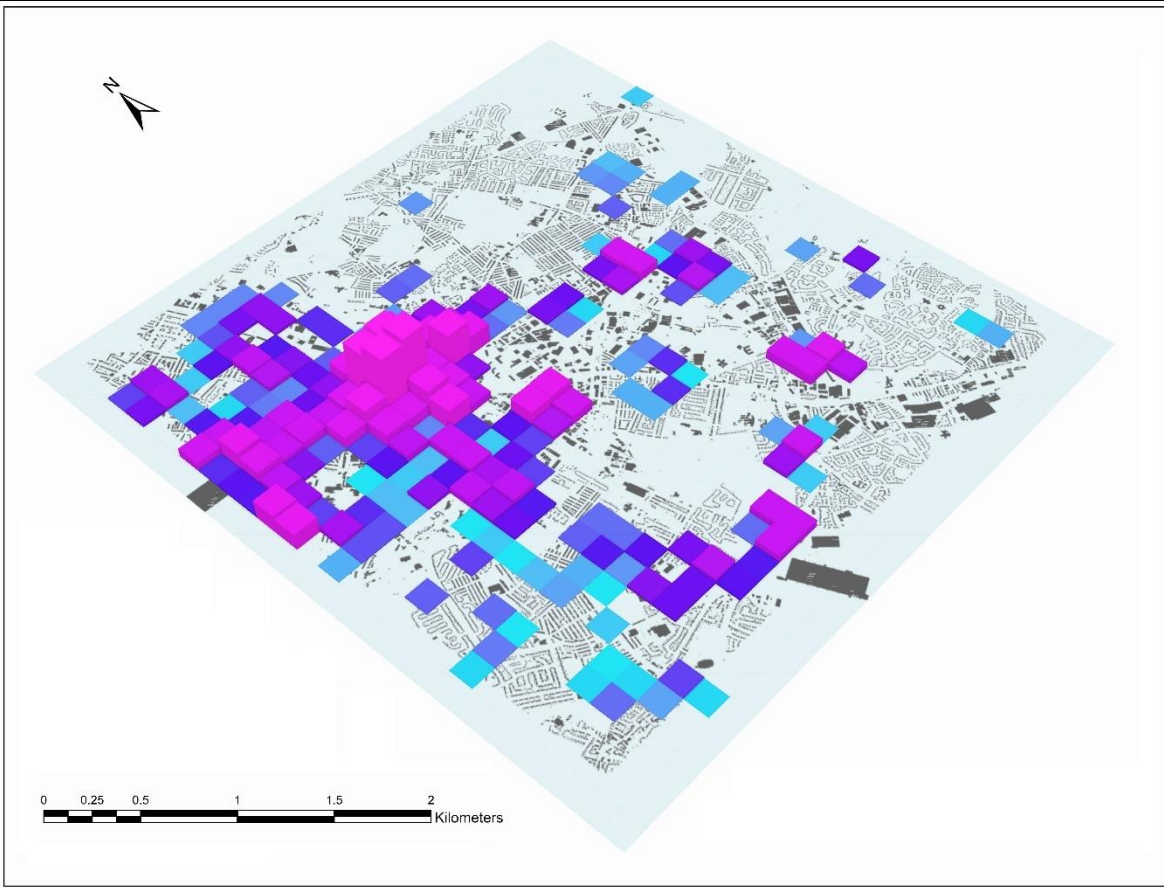
542 Representativeness of the MI for the buildings of the case study area were also
543 validated by applying the MI to a few exemplar sample buildings of the case study
544 area and then studying their structure individually. Details of this validation are
545 provided in supplementary material S8.

546 **4. Results and discussion:**

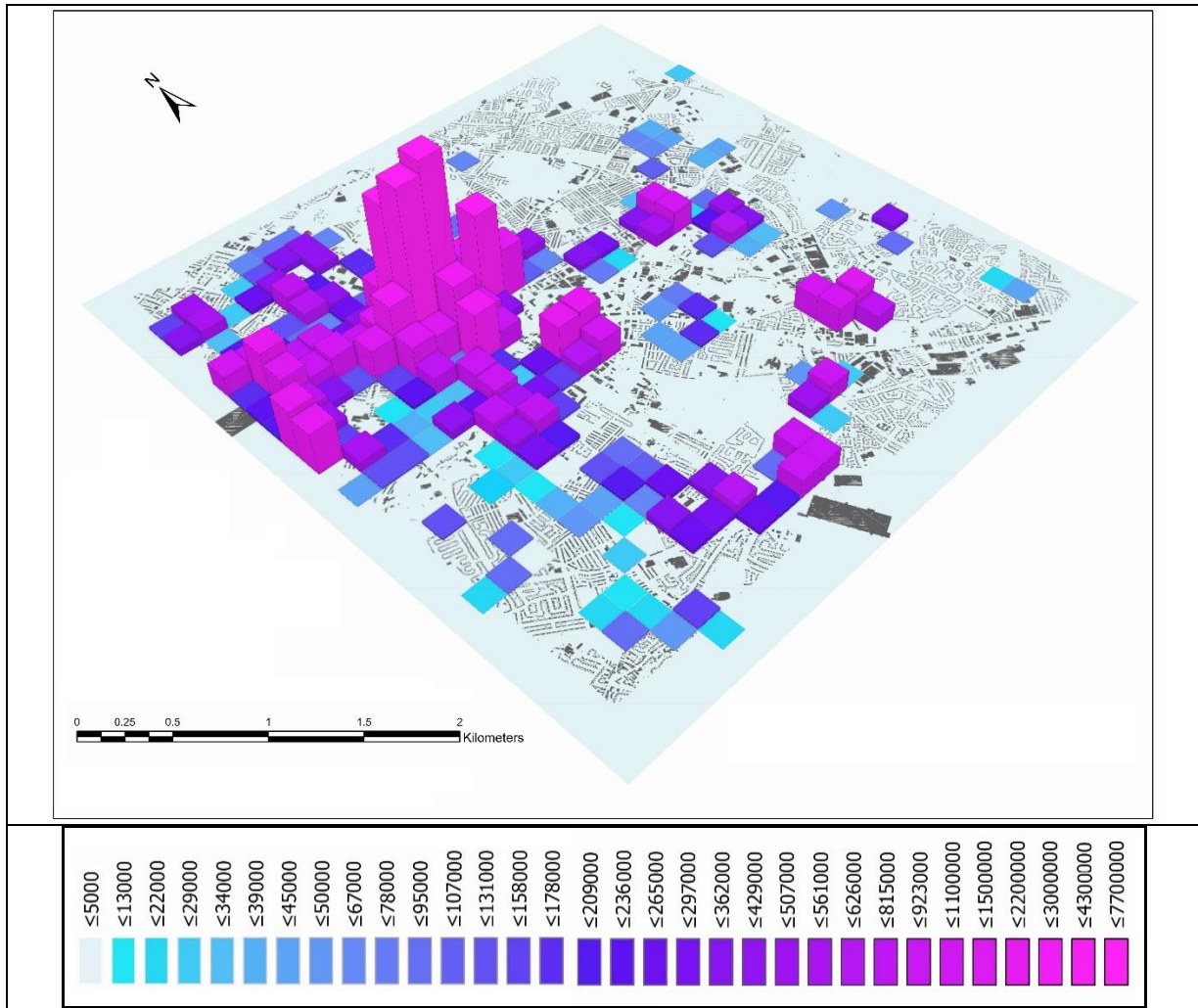
547 The results of method 1 are demonstrated as stacked volumes of steel and concrete
548 (Figure 6). For better observation, the results are rasterised into 200*200 m² cells
549 where all quantities of materials are aggregate into a single value for each cell. The
550 visualisation shows that there are large concentrations of both steel and concrete
551 within the Northwest of the city, while there are little steel and concrete on the East.
552 It must be noted that while only the quantities of steel and concrete of the selected
553 buildings are visualised in the maps, the footprints of all buildings are included as a
554 reference for the built-up areas.

555

Concrete Framed



Steel Framed



557 *Figure 6: Visualisation of rasterised urban stocks of concrete (above) and*
 558 *steel (below). The volumes are exaggerated two thousand-fold or better*
 559 *visualisation.*

560 Method 2 is applied by incorporating the temporal variations in the shares of steel-
 561 frame and concrete-frame multi-storey buildings. This would result in specifying steel
 562 and concrete into four different components. For the case study area, the total
 563 quantities of materials along with the GWPs that are calculated via method 2 are
 564 presented in table 7.

565 *Table 7: Quantities of in-use construction products and their associated*
 566 *GWPs calculated according to method 2.*

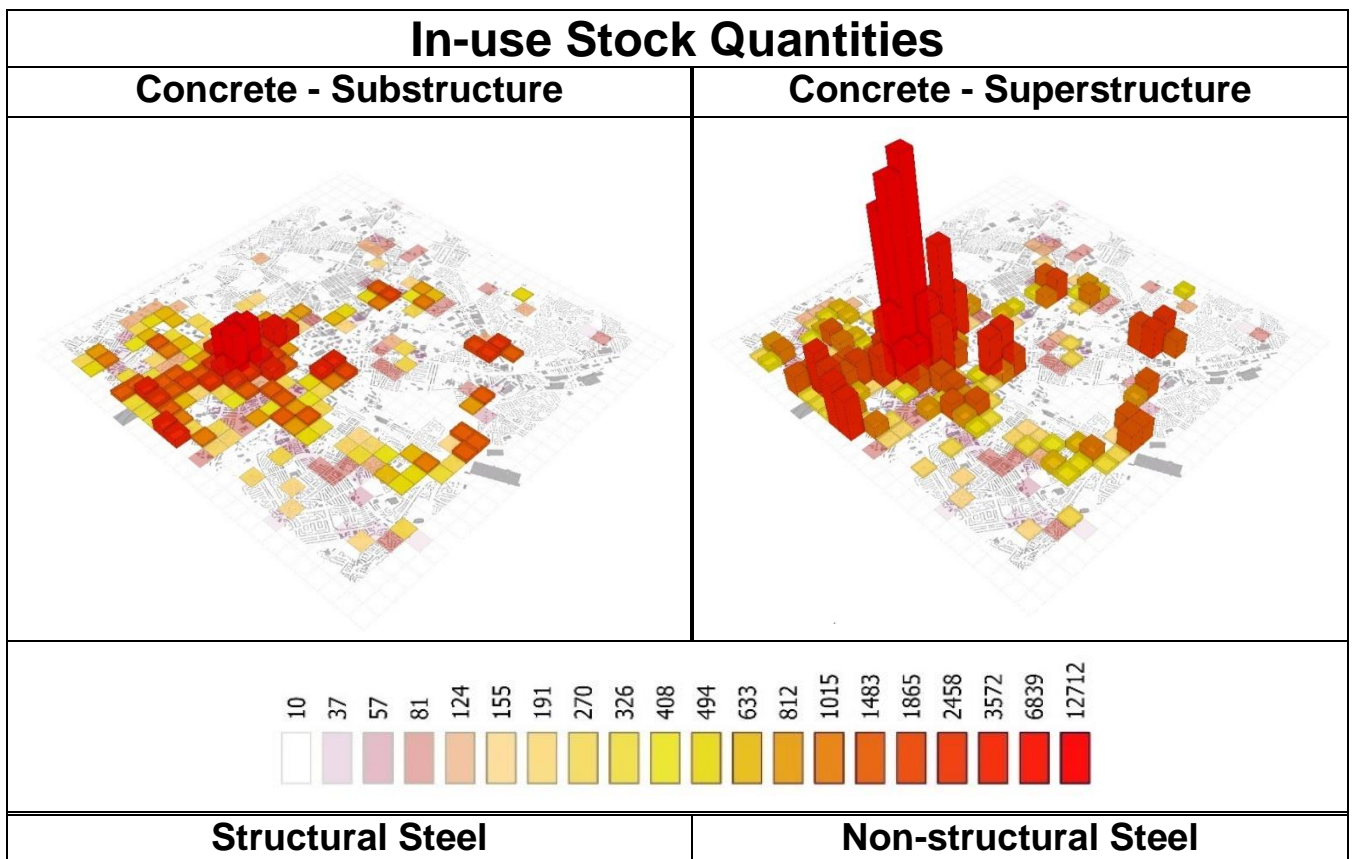
Quantities (m³ for concrete, tonnes for steel)				
Building classes	Substructure Concrete	Superstructure Concrete	Non-structural Steel	Structural Steel
Office	30,44	135,51	13,003	11,390
Commercial Core	74,19	335,37	33,981	17,693
High Rise	5,77	25,94	2,575	1,681

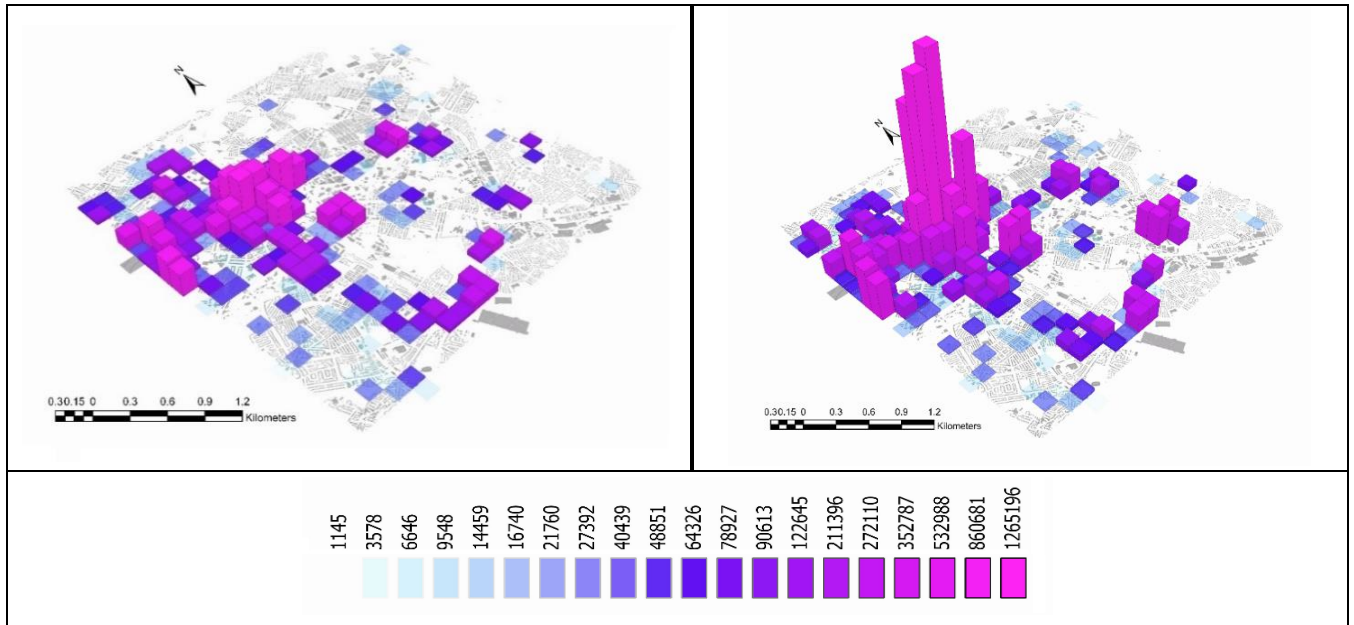
Low Rise	5,334	24,159	2,464	1,174
GWP (kt CO₂eq)				
Building classes	Substructure Concrete	Superstructure Concrete	Non-structural Steel	Structural Steel
Office	10.11	33.56	25.06	25.38
Commercial Core	24.63	83.06	65.48	39.42
High Rise	1.92	6.43	4.96	3.75
Low Rise	1.77	5.98	4.75	2.62

567

568 For visualisation, the results are initially granular as the MI of each year is applied to
569 the relevant buildings on the map. However, it should be noted that method 2
570 provides a representative MI for each year by considering the ‘probabilities’ of any
571 individual building to belong to one frame type. So, the MI is constructed as a
572 combination of the two frame types based on this probability. Thus, considering that
573 in reality a single building belongs to one of the frame types, method 3 cannot be
574 reliable at the resolution of individual buildings. To overcome this limitation, the
575 results are rasterised to avoid misrepresentation. The results are mapped
576 volumetrically in 200*200m cells to show the areas where there is a concentration of
577 each product (Figure 7).

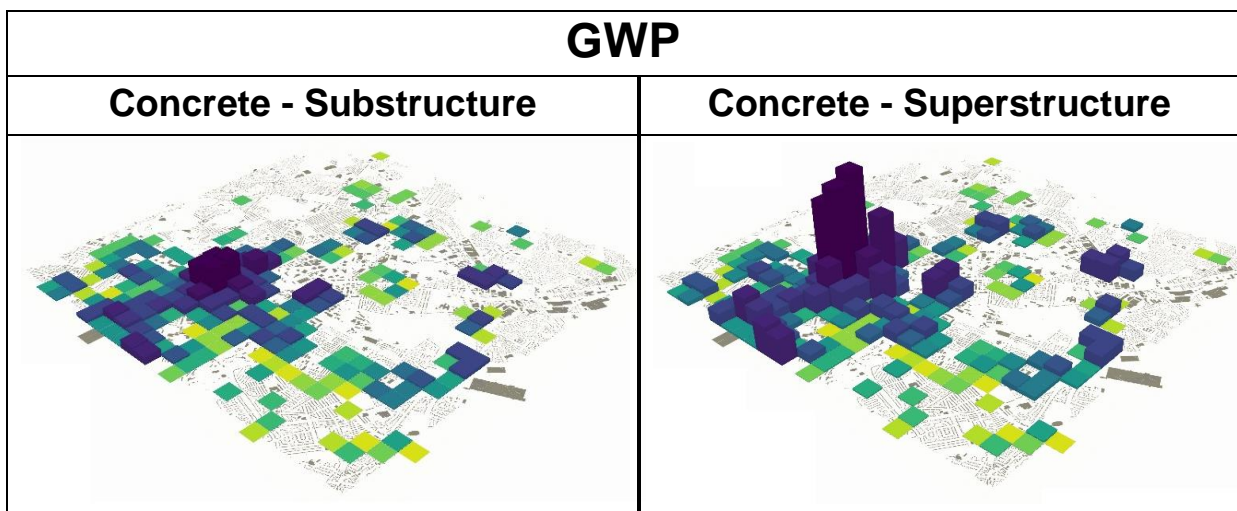
578

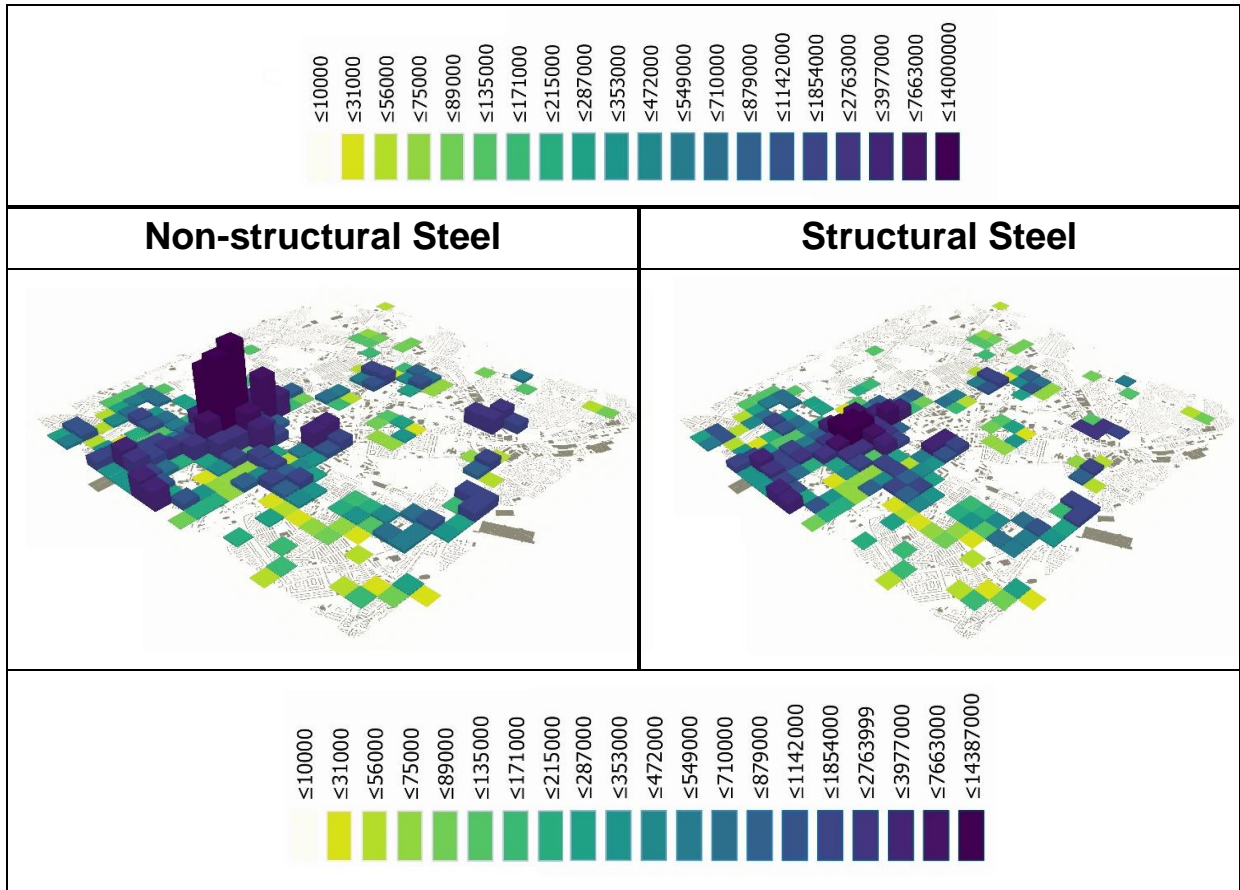




579 *Figure 7: Quantities of steel and concrete estimated via method 2*
 580 *characterised by type of products. The numbers are in m³ and kg*
 581 *respectively. The concrete volumes are exaggerated 2000 times for better*
 582 *visibility. For steel, each m³ of the prism bars represents 2 tonnes of steel.*

583 Similarly, the GWP are calculated for the modelled construction products as it was
 584 described in the methodology section. The results assign an embodied carbon to the
 585 four specified products of each individual building. This signifies that if the in-use
 586 stock is to be replaced with new similar products today, an equal amount of GHG
 587 emission will be released. The total embodied GWP of the case study are presented
 588 in table 7. For better visualisation, the GWP results are rasterised in 200m×200m
 589 cells. For each cell, the total amount of GWP of the construction for each product are
 590 specified and demonstrated with colour codes in Figure 8.





591

592 *Figure 8: summary of results of analysing GWP of the case study spatial*
 593 *model with method 2. The values are in kg CO₂eq.*

594 The aggregated results of the methods for the case study area are presented in table
 595 8.

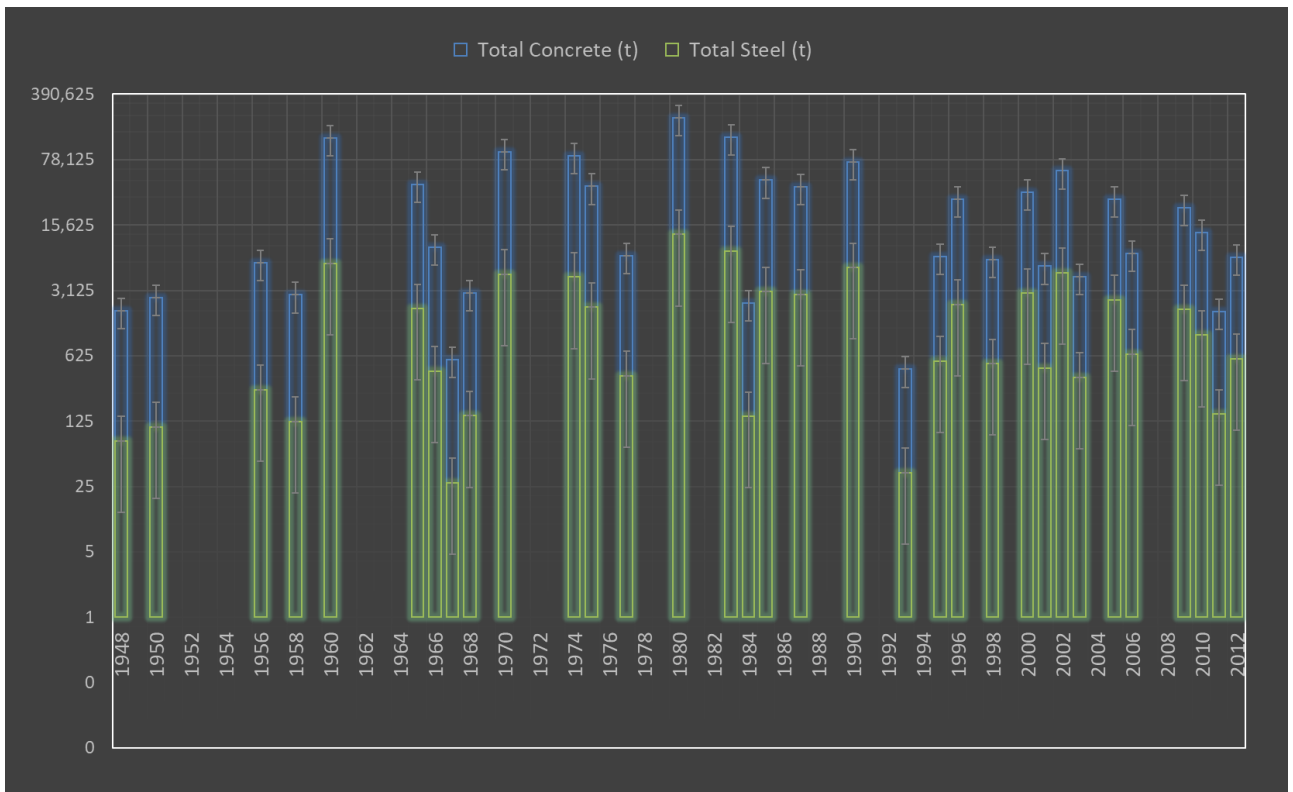
596 *Table 8: Comparison between the results of the two methods*

	Steel (tonnes)		Concrete (m ³)		GWP Steel (ktCO ₂ eq)	GWP concrete (ktCO ₂ eq)
Method 1	120,200		949,571		-	-
Method 2	Structural	Non-structural	Superstructure	Substructure	171.41	167.46
	31,940	52,025	521,003	115,746		
	83,965		636,748			

597

598 The histogram of the added stocks based on method 2 are visualised as bar chart
 599 from 1920 to 2018 (figure 9). The figure shows there has been a spike in
 600 accumulation of steel and concrete to the urban in-use stock from 1960 to 1990

601 possibly due to a period of increased construction of multi-storey buildings. There is
 602 a noticeable peak in 1980 after which the annual rate of added materials has been
 603 declining almost constantly.



604
 605 *Figure 9: Historical addition of steel and concrete (both in tonnes) to the in-*
 606 *use stock*

607 **5. Discussion:**

608 This study is the first attempt to model in-use structural steel and concrete at urban
 609 level by distinguishing between construction frame types. Technical feasibility and
 610 practical modelling efforts can be applied and specified to a variety of regions.
 611 Results are presented at high resolution which enables estimating quantities of steel
 612 and concrete as well as some key qualitative aspects such as approximate location,
 613 age, type of product, function of building, structure dimensions, and GWP.

614 The stock-flow model described estimates the spatial and temporal distribution of in-
 615 situ stocks of concrete and steel from 1945-present for over 2200 individual multi-
 616 story buildings in a 5km-by-5km area of one UK city. These buildings range in height
 617 from 6.1m to 23.5m with a total GFA of nearly 1.8 million m² and a total volume of 5
 618 million m³. As such it is the largest survey of building steel and concrete MI in the
 619 world. The total embodied carbon associated with concrete is 167.46 kt CO₂eq with
 620 steel is 171.41 kt CO₂eq.

621 Method2 provides an overall assessment of in-situ structural frame steel versus
 622 rebar steel and differentiates superstructure (frame, walls, and flooring) and

623 substructure (foundation and ramp) concrete. Superstructure concrete which
624 contains the major opportunity for product and material reclaim constitutes 82% of
625 the total quantity relative to the substructure across the four building types.
626 Superstructure concrete accounts for 77% of the embodied carbon across the four
627 classes of building. Structural steel – primarily the frame, comprises 42% of the total
628 steel relative to the four building types. Substructure concrete accounts for 23% of
629 the embodied carbon within the total embodied carbon across the four classes of
630 building. In total in-situ concrete and steel constitute around 84,000 tonnes of steel,
631 635 thousand m³ of concrete (approx. 1.6Mt) and an embodied GWP of 338 kt
632 CO₂eq. As a comparison total UK steel production in 2018 was 7 million tonnes and
633 concrete building products were 60 million tonnes (National Statistics, 2019).

634 The wide variation in MI found in previous studies highlights the need to develop
635 spatially explicit MI on case-by-case basis. It must be noted that the archetypes that
636 were presented in this study were simplified with the aim of increasing practicality
637 and the variations in different designs of each frame type over the decades must be
638 considered when interpreting the results. As data on structural frames of buildings is
639 not commonly available, the multi scenario spatiotemporal analysis of different
640 building frame types provide an opportunity to envisage georeferenced quantities of
641 material stocks when assuming different scenarios. The systematic model developed
642 in this study can be applied to thousands of buildings making large scale
643 assessment possible. The two methods calculated steel and concrete MI in two
644 different ways but as can be seen in Table 5 produce results within 5% variation.
645 Method2 however provides a basis for calculating primary MI of separate
646 superstructure and substructure materials. The aggregated results of method 2 are
647 expected to be more precise compared to method 1 as the impact of temporal trends
648 in construction practices are implemented in the method. In the absence of building
649 plans or other data on construction details Method 2 provides a step forward in
650 urban-scale assessment of qualities, quantities, and locations of building structural
651 products.

652 The current study assumes that the relationship between volumes and quantities of
653 structural products is linear. In reality however, the choice of construction products
654 depends on many factors including architecture, loads, geographical environment, or
655 even market conditions at the time of construction. As this study used two
656 archetypes, increasing the numbers of archetypes can improve the quality of results.
657 As modelling archetypes is time consuming, there should be a focus on optimising
658 the archetype making efforts to be most representative of building types and
659 dimensions. For instance, spatial statistical analysis may provide information on the
660 dimensions that would be most representative of the studied constructions of the
661 case study region. The ‘Jenks natural breaks optimisation’ analysis is a type of
662 spatial statistical study of objects that is capable of identifying most representative
663 classification breaks as it seeks to minimise each class's average deviation from the

664 class mean, while maximising each class's deviation from the means of the other
665 groups.

666 Integration of BIM approaches can also support and enhance creation of the MI
667 datasets and provides an opportunity to generate component and product specific
668 MI. While providing an opportunity, BIM approaches are either focusing on
669 prospective buildings, or require significant data collection for individual buildings,
670 thus their availability is very limited.

671

672 **5. Conclusions:**

673 There is a growing need to have spatially explicit characterisation of the in-use
674 stocks of material and products in order to analyse prospective dynamics of stocks
675 and flows and to implement a circular economy. Moreover, strategic urban planning
676 and managing impacts of waste generation and climate change would benefit from
677 such model. Whilst the lack of building plans limits the ability to estimate precise
678 dimensions of structural steel or concrete products, the proposed method using
679 archetypes provides a means to differentiate between structural and non-structural
680 components and focus attention on the significant volume and number of in-situ
681 structural components within urban areas available for future urban mining.

682 The urban-scale embodied carbon of the in-use built environment has rarely been
683 studied at spatial high resolution and product specification. While there is a growing
684 need to account for and spatialise it considering the growing concerns about climate
685 change and strategies aiming for reducing future carbon emissions. This study
686 improved the assessment of the embodied carbon of the built environment by
687 implementing the temporal pattern of construction types into the analysis.
688 Distinguishing between steel and concrete products that have different functions
689 allowed a more precise assessment of the embodied carbon.

690 **Acknowledgements**

691 This work was supported by the Engineering and Physical Sciences Research
692 Council (EPSRC) research grant 'REBUILD - REgenerative BUILDings and products
693 for a circular economy' [Grant reference: EP/P008917/1].

694

695

696 **6. References:**

- 697 Ajayebi, A., Hopkinson, P., Zhou, K., Lam, D., Chen, H.-M., Wang, Y., 2020.
698 Spatiotemporal model to quantify stocks of building structural products for a
699 prospective circular economy. *Resour. Conserv. Recycl.* 162, 105026.
700 <https://doi.org/10.1016/J.RESCONREC.2020.105026>
- 701 Augiseau, V., Barles, S., 2017. Studying construction materials flows and stock: A
702 review. *Resour. Conserv. Recycl.* 123, 153–164.
703 <https://doi.org/10.1016/J.RESCONREC.2016.09.002>
- 704 BCSA, 2019. British Constructional Steelwork Association Annual Review.
- 705 BEIS, 2020. building materials and components statistics April 2020.
- 706 Brütting, J., Desruelle, J., Senatore, G., Fivet, C., 2019. Design of Truss Structures
707 Through Reuse. *Structures* 18, 128–137.
708 <https://doi.org/10.1016/J.ISTRUC.2018.11.006>
- 709 BS, 2011. British Standard EN 15978:2011: Sustainability of construction works.
710 Assessment of environmental performance of buildings. Calculation method.
- 711 Cang, Y., Luo, Z., Yang, L. and Han, B., 2020. A new method for calculating the
712 embodied carbon emissions from buildings in schematic design: Taking
713 “building element” as basic unit. *Building and Environment*, 185, p.107306.
- 714 Dimoudi, A., Tompa, C., 2008. Energy and environmental indicators related to
715 construction of office buildings. *Resour. Conserv. Recycl.* 53, 86–95.
716 <https://doi.org/10.1016/J.RESCONREC.2008.09.008>
- 717 English Housing Survey, 2018. English Housing Survey, National Statistics.
- 718 Enviromate, 2020. buy, sell & discover leftover building materials [WWW Document].
719 URL <https://www.enviromate.co.uk/>
- 720 Excess materials exchange, 2020. Excess materials exchange [WWW Document].
721 URL <https://excessmaterialsexchange.com/nl/>
- 722 Gallego-Schmid, A., Chen, H.-M., Sharmina, M., Mendoza, J.M.F., 2020. Links
723 between circular economy and climate change mitigation in the built
724 environment. *J. Clean. Prod.* 260, 121115.
725 <https://doi.org/10.1016/J.JCLEPRO.2020.121115>
- 726 Gontia, P., Nägeli, C., Rosado, L., Kalmykova, Y., Österbring, M., 2018. Material-
727 intensity database of residential buildings: A case-study of Sweden in the
728 international context. *Resour. Conserv. Recycl.* 130, 228–239.
729 <https://doi.org/10.1016/J.RESCONREC.2017.11.022>
- 730 Graedel, T.E., Allwood, J., Birat, J.-P., Buchert, M., Hagelüken, C., Reck, B.K.,
731 Sibley, S.F., Sonnemann, G., 2011. What Do We Know About Metal Recycling
732 Rates? *J. Ind. Ecol.* 15, 355–366. [https://doi.org/10.1111/j.1530-](https://doi.org/10.1111/j.1530-9290.2011.00342.x)
733 [9290.2011.00342.x](https://doi.org/10.1111/j.1530-9290.2011.00342.x)
- 734 Gregory, R.J., Hughes, T.G., Kwan, A.S.K., 2004. Brick recycling and reuse. *Proc.*

- 735 Inst. Civ. Eng. - Eng. Sustain. 157, 155–161.
736 <https://doi.org/10.1680/ensu.2004.157.3.155>
- 737 Haas, W., Krausmann, F., Wiedenhofer, D., Lauk, C., Mayer, A., 2020. Spaceship
738 earth's odyssey to a circular economy - a century long perspective. *Resour.*
739 *Conserv. Recycl.* 163, 105076.
740 <https://doi.org/10.1016/J.RESCONREC.2020.105076>
- 741 Han, J., Xiang, W.-N., 2013. Analysis of material stock accumulation in China's
742 infrastructure and its regional disparity. *Sustain. Sci.* 8, 553–564.
743 <https://doi.org/10.1007/s11625-012-0196-y>
- 744 Heeren, N., Fishman, T., 2019. A database seed for a community-driven material
745 intensity research platform. *Sci. Data* 6, 23. [https://doi.org/10.1038/s41597-019-](https://doi.org/10.1038/s41597-019-0021-x)
746 [0021-x](https://doi.org/10.1038/s41597-019-0021-x)
- 747 Krausmann, F., Wiedenhofer, D., Lauk, C., Haas, W., Tanikawa, H., Fishman, T.,
748 Miatto, A., Schandl, H., Haberl, H., 2017. Global socioeconomic material stocks
749 rise 23-fold over the 20th century and require half of annual resource use. *Proc.*
750 *Natl. Acad. Sci.* 114, 1880–1885. <https://doi.org/10.1073/PNAS.1613773114>
- 751 Lanau, M., Liu, G., Kral, U., Wiedenhofer, D., Keijzer, E., Yu, C., Ehlert, C., 2019.
752 Taking Stock of Built Environment Stock Studies: Progress and Prospects.
753 *Environ. Sci. Technol.* 53, 8499–8515. <https://doi.org/10.1021/acs.est.8b06652>
- 754 Mastrucci, A., Marvuglia, A., Popovici, E., Leopold, U., Benetto, E., 2017. Geospatial
755 characterization of building material stocks for the life cycle assessment of end-
756 of-life scenarios at the urban scale. *Resour. Conserv. Recycl.* 123, 54–66.
757 <https://doi.org/10.1016/J.RESCONREC.2016.07.003>
- 758 Miatto, A., Schandl, H., Forlin, L., Ronzani, F., Borin, P., Giordano, A., Tanikawa, H.,
759 2019. A spatial analysis of material stock accumulation and demolition waste
760 potential of buildings: A case study of Padua. *Resour. Conserv. Recycl.* 142,
761 245–256. <https://doi.org/10.1016/J.RESCONREC.2018.12.011>
- 762 Moynihan, M.C., Allwood, J.M., 2014. Utilization of structural steel in buildings. *Proc.*
763 *R. Soc. A Math. Phys. Eng. Sci.* 470, 20140170.
764 <https://doi.org/10.1098/rspa.2014.0170>
- 765 MPA, 2018. Mineral Products Association Sustainable Development Report 2018.
- 766 National Statistics, 2019. Monthly Statistics of Building Materials & Components-
767 April 2019.
- 768 Ortlepp, R., Gruhler, K., Schiller, G., 2018. Materials in Germany's domestic building
769 stock: calculation model and uncertainties. *Build. Res. Inf.* 46, 164–178.
770 <https://doi.org/10.1080/09613218.2016.1264121>
- 771 Ortlepp, R., Gruhler, K., Schiller, G., 2016. Material stocks in Germany's non-
772 domestic buildings: a new quantification method. *Build. Res. Inf.* 44, 840–862.
773 <https://doi.org/10.1080/09613218.2016.1112096>
- 774 Pomponi, F., Moncaster, A., 2017. Circular economy for the built environment: A
775 research framework. *J. Clean. Prod.* 143, 710–718.

- 776 <https://doi.org/10.1016/J.JCLEPRO.2016.12.055>
- 777 Rocks, L., 2020. Loop Rocks.
- 778 Romero Perez de Tudela, A., Rose, C.M., Stegemann, J.A., 2020. Quantification of
779 material stocks in existing buildings using secondary data—A case study for
780 timber in a London Borough. *Resour. Conserv. Recycl.* X 5, 100027.
781 <https://doi.org/10.1016/J.RCRX.2019.100027>
- 782 Salvo, 2020. Salvo - reuse for the world you want [WWW Document]. URL
783 <https://www.salvoweb.com/about>
- 784 Sansom, M., Avery, N., 2014. Briefing: Reuse and recycling rates of UK steel
785 demolition arisings. *Proc. Inst. Civ. Eng. - Eng. Sustain.* 167, 89–94.
786 <https://doi.org/10.1680/ensu.13.00026>
- 787 Schebek, L., Schnitzer, B., Blesinger, D., Köhn, A., Miekley, B., Linke, H.J.,
788 Lohmann, A., Motzko, C., Seemann, A., 2017. Material stocks of the non-
789 residential building sector: the case of the Rhine-Main area. *Resour. Conserv.*
790 *Recycl.* 123, 24–36. <https://doi.org/10.1016/J.RESCONREC.2016.06.001>
- 791 Stephan, A., Athanassiadis, A., 2017a. Towards a more circular construction sector:
792 Estimating and spatialising current and future non-structural material
793 replacement flows to maintain urban building stocks.
794 <https://doi.org/10.1016/j.resconrec.2017.09.022>
- 795 Stephan, A., Athanassiadis, A., 2017b. Quantifying and mapping embodied
796 environmental requirements of urban building stocks. *Build. Environ.* 114, 187–
797 202. <https://doi.org/10.1016/J.BUILDENV.2016.11.043>
- 798 Streeck, J., Wiedenhofer, D., Krausmann, F., Haberl, H., 2020. Stock-flow relations
799 in the socio-economic metabolism of the United Kingdom 1800–2017. *Resour.*
800 *Conserv. Recycl.* 161, 104960.
801 <https://doi.org/10.1016/J.RESCONREC.2020.104960>
- 802 Tanikawa, H., Hashimoto, S., 2009. Urban stock over time: spatial material stock
803 analysis using 4d-GIS. *Build. Res. Inf.* 37, 483–502.
804 <https://doi.org/10.1080/09613210903169394>
- 805 Wang, T., Müller, D.B., Hashimoto, S., 2015. The Ferrous Find: Counting Iron and
806 Steel Stocks in China's Economy. *J. Ind. Ecol.* 19, 877–889.
807 <https://doi.org/10.1111/jiec.12319>
- 808 Wiedenhofer, D., Fishman, T., Lauk, C., Haas, W., Krausmann, F., 2019. Integrating
809 Material Stock Dynamics Into Economy-Wide Material Flow Accounting:
810 Concepts, Modelling, and Global Application for 1900–2050. *Ecol. Econ.* 156,
811 121–133. <https://doi.org/10.1016/J.ECOLECON.2018.09.010>
- 812 Wiedenhofer, D., Steinberger, J.K., Eisenmenger, N., Haas, W., 2015. Maintenance
813 and Expansion: Modeling Material Stocks and Flows for Residential Buildings
814 and Transportation Networks in the EU25. *J. Ind. Ecol.* 19, 538–551.
815 <https://doi.org/10.1111/jiec.12216>
- 816 Xing, S., Xu, Z., Jun, G., 2008. Inventory analysis of LCA on steel- and concrete-

817 construction office buildings. Energy Build. 40, 1188–1193.
818 <https://doi.org/10.1016/j.enbuild.2007.10.016>